

# Exclusive dipion production

Justyna Tomaszewska on behalf of the ZEUS Collaboration

Universität Hamburg, Luruper Chaussee 149, D-22761 Hamburg

DOI: <http://dx.doi.org/10.3204/DESY-PROC-2012-02/38>

The exclusive electroproduction of two pions in the mass range  $0.4 < M_{\pi\pi} < 2.5$  GeV has been studied with the ZEUS detector at HERA using an integrated luminosity of  $82 \text{ pb}^{-1}$ . The two-pion invariant-mass distribution is interpreted in terms of the pion electromagnetic form factor,  $|F(M_{\pi\pi})|$ , assuming that the studied mass range includes the contributions of the  $\rho$ ,  $\rho'$  and  $\rho''$  vector-meson states.

## 1 Exclusive dipion production

Exclusive electroproduction of vector mesons takes place through a virtual photon  $\gamma^*$  by means of the process  $\gamma^* p \rightarrow V p$ . At large values of the centre-of-mass energy,  $W$ , this is usually viewed as a three-step process; the virtual photon  $\gamma^*$  fluctuates into a  $q\bar{q}$  pair which interacts with the proton through a two-gluon ladder and hadronizes into a vector meson,  $V$ .

Exclusive  $\pi^+\pi^-$  production has been measured at HERA [1] experiments: ZEUS [2, 3] and H1 [4] as well as in the annihilation process  $e^+e^- \rightarrow \pi^+\pi^-$  [5, 6]. The  $\pi^+\pi^-$  mass distribution shows a complex structure in the mass range 1–2 GeV. Evidence for two excited vector-meson states has been established [7]; the  $\rho'(1450)$  is assumed to be predominantly a radially excited  $2S$  state and the  $\rho''(1700)$  is an orbitally excited  $2D$  state, with some mixture of the  $S$  and  $D$  waves [8]. In addition there is also the  $\rho_3(1690)$  spin-3 meson [9] which has a  $\pi\pi$  decay mode.

### 1.1 Data selection

The data used in this analysis were collected at the HERA ep collider during 1998–2000 with the ZEUS detector. At that time HERA operated at a proton energy of 920 GeV and at a positron energy of 27.5 GeV. The integrated luminosity used was  $82 \text{ pb}^{-1}$ .

The data are selected in the two-pion mass range  $0.4 < M(\pi\pi) < 2.5$  GeV, in the kinematic range  $2.5 < Q^2 < 80 \text{ GeV}^2$ ,  $32 < W < 180 \text{ GeV}$  and  $|t| < 0.6 \text{ GeV}^2$ , where  $Q^2$  is the virtuality of the photon and  $t$  is the squared four-momentum transfer at the proton vertex. The  $M_{\pi\pi}$  system consists of a resonance part and a non-resonant background.

### 1.2 Pion Form Factor

The resonances ( $\rho$ ,  $\rho'$  and  $\rho''$ ) are described by the pion form factor,  $F_\pi$ . It can be related to the  $\pi\pi$  invariant-mass distribution through the following relation [10]:

$$\frac{dN(M(\pi\pi))}{dM_{\pi\pi}} \propto |F_\pi(M_{\pi\pi})|^2$$

In the mass range  $M_{\pi\pi} < 2.5$  GeV, Kuhn-Santamaria (KS) [11] include contributions from the  $\rho(770)$ ,  $\rho'(1450)$  and  $\rho''(1700)$  resonances,

$$F_\pi = \frac{BW_\rho(M_{\pi\pi}) + \beta BW_{\rho'}(M_{\pi\pi}) + \gamma BW_{\rho''}(M_{\pi\pi})}{1 + \beta + \gamma}.$$

Here  $\beta$  and  $\gamma$  are relative amplitudes and  $BW_V$  is the Breit-Wigner distribution of the vector meson  $V$ .

The  $\pi^+\pi^-$  mass distribution, after acceptance correction, is shown in Figure 1. A clear peak is seen in the  $\rho$  mass range. A small shoulder is apparent around 1.3 GeV and a secondary peak at about 1.8 GeV.

The two-pion invariant-mass distribution was fitted, using the least-square method, as a sum of two terms,

$$\frac{dN(M_{\pi\pi})}{dM_{\pi\pi}} = A \left( 1 - \frac{4M_\pi^2}{M_{\pi\pi}^2} \right) \left[ F_\pi + B \left( \frac{M_0}{M_{\pi\pi}} \right)^n \right],$$

where  $A$  is an overall normalization constant. The second term is a parameterization of the non-resonant background, with constant parameters  $B$ ,  $n$  and  $M_0 = 1$  GeV. The other parameters, the masses and widths of the three resonances and their relative contributions  $\beta$  and  $\gamma$ , enter through the pion form factor,  $F_\pi$ . The fit, which includes 11 parameters, gives a good description of the data.

The result of the fit is shown in Figure 1 together with the contribution of each of the two terms. The  $\rho$  and the  $\rho''$  signals are clearly visible. The negative interference between all the resonances results in the  $\rho'$  signal appearing as a shoulder.

### 1.3 $Q^2$ dependence

The  $Q^2$  dependence of the relative amplitudes was determined by performing the fit to  $M_{\pi\pi}$  in three  $Q^2$  regions, 2–5, 5–10 and 10–80 GeV<sup>2</sup>. The results are shown in Figure 2. A reasonable description of the data is achieved in all three  $Q^2$  regions. The absolute value of  $\beta$  increases with  $Q^2$ , while the value of  $\gamma$  is consistent with no  $Q^2$  dependence, within large uncertainties.

The  $Q^2$  dependence of the  $\rho$  by itself is given elsewhere [2]. Since the  $\pi\pi$  branching ratios of  $\rho'$  and  $\rho''$  are poorly known, the ratio  $R_V$  defined as

$$R_V = \frac{\sigma(V) \cdot Br(V \rightarrow \pi\pi)}{\sigma(\rho)},$$

has been measured, where  $\sigma$  is the cross section for vector-meson production, and  $Br(V \rightarrow \pi\pi)$  is the branching ratio of the vector meson  $V(\rho', \rho'')$  into  $\pi\pi$ .

The ratio  $R_V$  for  $V = \rho', \rho''$ , as a function of  $Q^2$  is presented in Figure 3.

Owing to the large uncertainties of  $R_{\rho''}$ , no conclusion on its  $Q^2$  behaviour can be deduced, whereas  $R_{\rho'}$  clearly increases with  $Q^2$ . This rise has been predicted by several models [12, 13, 14, 15, 16]. The suppression of the  $2S$  state ( $\rho'$ ) is connected to a node effect, which results

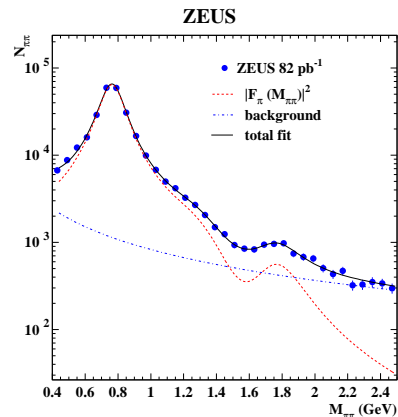


Figure 1: The two-pion invariant-mass distribution,  $M_{\pi\pi}$ , where  $N_{\pi\pi}$  is the acceptance-corrected number of events in each bin of 60 MeV. The dots are the data and the full line is the result of a fit using the Kuhn-Santamaria parameterization. The dashed line is the result of the pion form factor normalized to the data, and the dash-dotted line denotes the background contribution.

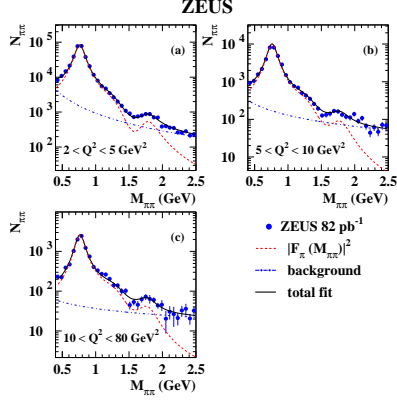


Figure 2: The two-pion invariant-mass distribution,  $M_{\pi\pi}$  for three regions of  $Q^2$ , as denoted in the figure.

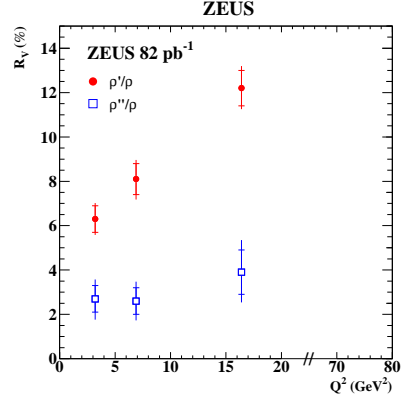


Figure 3: The ratio  $R_V$  as a function of  $Q^2$  for  $V = \rho'$  (full circles) and  $\rho''$  (open squares). The inner error bars indicate the statistical uncertainty, the outer error bars represent the statistical and systematic uncertainty added in quadrature.

in cancellations of contributions from different impact-parameter regions at lower  $Q^2$ , while at higher  $Q^2$  the effect vanishes.

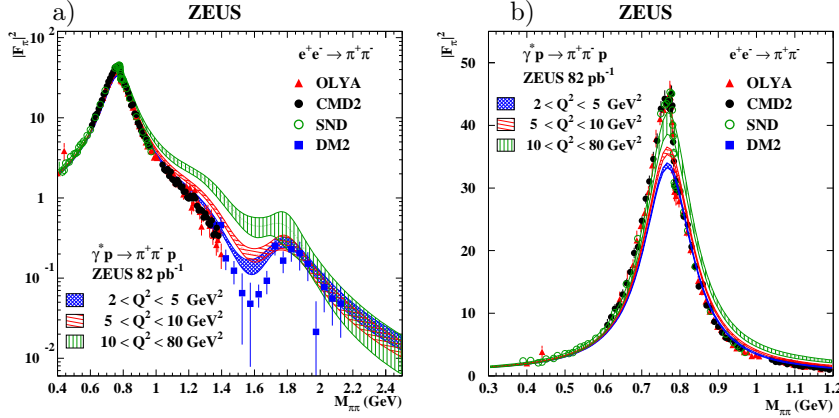


Figure 4: The pion form factor squared,  $|F_\pi|^2$ , in the whole mass range (a)) and in the  $\rho$  mass region (b)), as a function of the  $\pi^+\pi^-$  invariant mass,  $M_{\pi\pi}$ , as obtained from the reaction  $e^+e^- \rightarrow \pi^+\pi^-$  [5, 17, 18, 19, 20]. The shaded bands represent the square of the pion form factor and its total uncertainty obtained in the present analysis for three ranges of  $Q^2$ : 2–5  $\text{GeV}^2$  (crossed lines), 5–10  $\text{GeV}^2$  (horizontal lines) and 10–80  $\text{GeV}^2$  (vertical lines).

Figure 4 a) shows the curves representing the pion form factor,  $|F_\pi(M_{\pi\pi})|^2$ , as obtained in the present analysis for the three  $Q^2$  ranges: 2–5, 5–10, 10–80  $\text{GeV}^2$ . Also shown are results

obtained in the time-like regime from the reaction  $e^+e^- \rightarrow \pi^+\pi^-$ . In general, the features of the  $|F_\pi(M_{\pi\pi})|^2$  distribution observed here are also observed in  $e^+e^-$ , i.e., the prominent  $\rho$  peak, a shoulder around the  $\rho'$  and a dip followed by an enhancement in the  $\rho''$  region. Above the  $\rho$  region, where the interference between the  $\rho'$  and the  $\rho''$  starts to dominate, there is a dependence of  $|F_\pi(M_{\pi\pi})|^2$  on  $Q^2$ , with the results from the lowest  $Q^2$  range closest to those from  $e^+e^-$ . However, in the region of the  $\rho$  peak, shown in Figure 4 b), the pion form-factor  $|F_\pi(M_{\pi\pi})|^2$  is highest at the highest  $Q^2$ , as in the  $\rho'$ - $\rho''$  interference region, while the  $e^+e^-$  data are higher than those in the highest  $Q^2$  range. They are equal within errors for  $M_{\pi\pi} > 1.8$  GeV.

## 2 Summary

Exclusive two-pion electroproduction has been studied by ZEUS at HERA. The mass distribution is well described by the pion electromagnetic form factor,  $|F_\pi(M_{\pi\pi})|^2$ , which includes three resonances,  $\rho$ ,  $\rho'(1450)$  and  $\rho''(1700)$ .

A  $Q^2$  dependence of  $|F_\pi(M_{\pi\pi})|^2$  is observed, visible in particular in the interference region between  $\rho'$  and  $\rho''$ . The electromagnetic pion form factor obtained from the present analysis is lower (higher) than that obtained from  $e^+e^- \rightarrow \pi^+\pi^-$  for  $M_{\pi\pi} < 0.8$  GeV ( $0.8 < M_{\pi\pi} < 1.8$  GeV). They are equal within errors for  $M_{\pi\pi} > 1.8$  GeV.

The  $Q^2$  dependence of the cross-section ratios  $R_{\rho'} = \sigma(\rho' \rightarrow \pi\pi)/\sigma(\rho)$  and  $R_{\rho''} = \sigma(\rho'' \rightarrow \pi\pi)/\sigma(\rho)$ , has been studied. The ratio  $R_{\rho'}$  rises strongly with  $Q^2$ , as expected in QCD-inspired models in which the wave-function of the vector meson is calculated within the constituent quark model, which allows for nodes in the wave-function to be present.

## References

- [1] A Proposal for a Large Electron-Proton Colliding Beam Facility at DESY, DESY HERA 81-10 (1981).
- [2] ZEUS Coll., S. Chekanov et al., PMC Phys. **A 1** (2007) 6.
- [3] ZEUS Coll., H. Abramowicz et al., Eur. Phys. J. C **72** (2012) 1869.
- [4] H1 Coll., F.D. Aaron et al., JHEP **05** (2010) 032.
- [5] L.M. Barkov et al., Nucl. Phys. **B 256** (1985) 365.
- [6] D. Aston et al., Phys. Lett. **B 92** (1980) 215.
- [7] A. Donnachie and H. Mirzaie, Z. Phys. **C 33** (1987) 407.
- [8] I.P. Ivanov and N.N. Nikolaev, JETP Lett. **69** (1999) 294.
- [9] Omega Photon Coll., M. Atkinson et al., Z.Phys. **C 26** (1985) 499.
- [10] B. Clerbaux and M.V. Polyakov, Nucl. Phys. **A 79** (2000) 185.
- [11] J.H. Kuhn and A. Santamaria, Z. Phys. **C 48** (1990) 445.
- [12] J. Nemchik, N.N. Nikolaev and B.G. Zakharov, Phys. Lett. **B 339** (1994) 194.
- [13] L. Frankfurt, W. Koepf and M. Strikman, Phys. Rev. **D 54** (1996) 3194.
- [14] I.P. Ivanov and N.N. Nikolaev, Acta Phys. Polon. **B 33** (2002) 3517.
- [15] H. Abramowicz, L. Frankfurt and M. Strikman, Surveys High Energy Phys. **11** (1997) 51.
- [16] I.P. Ivanov, PhD Thesis (Bonn University), hep-ph/0303035 (2003).
- [17] DM2 Coll., D. Bisello et al., Phys. Lett. **B 220** (1989) 312.
- [18] CMD2 Coll., R.R. Akhmetshin et al., Phys. Lett. **B 527** (2002) 161.
- [19] CMD2 Coll. V.M. Aul'chenko et al., JETP Lett., **82** (2005) 743.
- [20] SND Coll., M.N. Achasov et al., J. Exp. Theor. Phys. **101** (2005) 1053.